

T. V. Nguyen

Student Mem. ASME.

C. Brennen

Associate Professor of Mechanical Engineering,
Mem. ASME

R. H. Sabersky

Professor of Mechanical Engineering,
Mem. ASME

Division of Engineering and
Applied Science 104-44,
California Institute of Technology,
Pasadena, Calif. 91125

Gravity Flow of Granular Materials in Conical Hoppers

An approximate solution to the flow of a cohesionless granular material in a conical hopper is presented. The material is modeled as a perfectly plastic continuum which satisfies the Mohr-Coulomb yield condition. Analytical expressions of the mass flow rate and the wall stress are derived and compared to some experimental data and other analyses.

Introduction

This paper presents an approximate solution to the flow of a cohesionless granular material in a conical hopper. This is a problem which has received considerable attention in the past though much of the work was directed toward developing an empirical relation of the mass flow rate from experimental data (for example [1, 2]). In the early 1960's Jenike and Johanson [23] applied the basic principles of plasticity to study the behavior of bulk solids; the material was treated as a perfectly plastic solid which yields according to the Mohr-Coulomb condition. Jenike [3] solved the equilibrium equations in a hopper with a "radial stress field;" that is to say the mean stress in the material was assumed to vary linearly with the radial distance from the apex of the hopper. However, no unique velocity field can be derived from such a quasi-static analysis; the addition of inertia is necessary in order to obtain a unique velocity field. Unfortunately, the resulting nonlinear equations of motion are considerably more difficult to solve.

Brown [4] studied the problem using an energy approach. He assumed that the material would flow when the total kinetic and potential energies are at a minimum. From this, he derived an expression for the mass flow rate. Savage [5] used a perturbation scheme based on the wall friction angle to solve the problem of flow in a hopper. Up to the order presented, the velocity and stress field are weak functions of the angular position θ (see Fig. 1). Brennen and Pearce [6] solved the problem for a two-dimensional hopper. They used a perturbation scheme based on the angular position θ , introduced modified

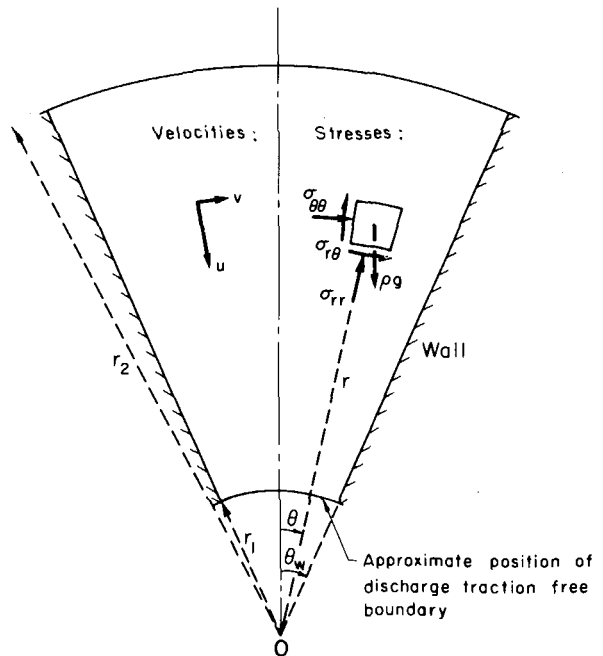


Fig. 1 Schematic for conical hopper flow

Contributed by the Applied Mechanics Division for presentation at the Winter Annual Meeting, New York, N. Y., December 2-7, 1979, of THE AMERICAN SOCIETY OF MECHANICAL ENGINEERS.

Discussion on this paper should be addressed to the Editorial Department, ASME, United Engineering Center, 345 East 47th Street, New York, N. Y. 10017, and will be accepted until December 1, 1979. Readers who need more time to prepare a Discussion should request an extension of the deadline from the Editorial Department. Manuscript received by ASME Applied Mechanics Division, July, 1978; final revision, April, 1979. Paper No. 79-WA/APM-20.

boundary conditions at the upper and lower discharge surfaces and found that the free surface at the hopper exit did not coincide precisely with the cylindrical surface at the exit radius. It took the shape of an arch which spanned the outlet. The resulting theoretical mass flow rates were in good agreement with the experiments for hoppers with half angles up to 40° . Davidson and Nedderman [7] obtained analytical expressions of the velocity and stress distribution in a

hopper. Their solution assumed that the shear stress was equal to zero and that the body force was in the radial direction. This solution then gave an upper limit to the flow rate. Sullivan [8] solved the same problem in his unpublished thesis. Williams [9] derived the upper and lower limits of the flow rate by solving the flow equations on the center line and along the hopper wall, respectively. This solution contains some assumptions which are quite severe.

Another quantity which is important in the design of hoppers is the stress which the material exerts on the hopper wall. It is widely known that the wall stress pattern when the material is flowing is very different from the one which exists when the material is at rest in the hopper. This is usually attributed to a switch from the active stress field in the static material to a passive one in the flowing material. Walker [10] presented an approximate analysis of the stress on the hopper wall by considering the force balance on a volume of material. Similar work was done by Walters [11]. Jenike and Johanson [12-15] presented a fairly complete analysis of the bin loads. They clearly defined the different stress fields which exist in the hopper during the filling and the flowing periods. Recently, Cowin [17] analyzed the wall stresses in a vertical bin and concluded that the Janssen formula gave only the lower limits of the possible wall stress values.

An approximate solution for conical hoppers which is based on a perturbation scheme is presented in this paper and comparison is made with experiments.

The Equations of Flow

The geometry of the problem is presented in Fig. 1. A spherical coordinate system is used to represent the axisymmetric flow field. The unknowns are the velocity components u and v in the $-r$ and $-\theta$ direction, respectively, the normal stresses σ_r , σ_θ , σ_α in the r , θ , α directions and the shear stress $\sigma_{r\theta}$. Compressive stresses were taken to be positive.

The material is assumed to have a constant density during the flow; its void ratio is therefore constant at the critical value when yielding initially occurs during startup. This incompressibility condition is supported by Jenike [3] and Jenike and Shield [18].

The continuity equation is written as

$$\frac{\partial u}{\partial r} + 2\frac{u}{r} + \frac{1}{r}\frac{\partial v}{\partial \theta} + \frac{v}{r}\cot\theta = 0 \quad (1)$$

The equations of motion in spherical coordinates are

$$\frac{\partial \sigma_r}{\partial r} + \frac{1}{r}\frac{\partial \sigma_{r\theta}}{\partial \theta} + \frac{1}{r}[2\sigma_r - \sigma_\theta - \sigma_\alpha + \sigma_{r\theta}\cot\theta] + \gamma\cos\theta = -\rho\left[u\frac{\partial u}{\partial r} + \frac{v}{r}\frac{\partial u}{\partial \theta} - \frac{v^2}{r}\right] \quad (2)$$

in the radial direction and

$$\frac{\partial \sigma_{r\theta}}{\partial r} + \frac{1}{r}\frac{\partial \sigma_\theta}{\partial \theta} + \frac{1}{r}[(\sigma_\theta - \sigma_\alpha)\cot\theta + 3\sigma_{r\theta}] - \gamma\sin\theta = -\rho\left[u\frac{\partial v}{\partial r} + \frac{v}{r}\frac{\partial v}{\partial \theta} + \frac{uv}{r}\right] \quad (3)$$

in the tangential direction.

Two constitutive relations of the material are needed. They are the yield condition and the isotropy condition.

As Jenike [3] has pointed out, the development of a yield function is a major difficulty in the study of bulk solids. Attempts have been made to adapt the Tresca and Von Mises yield functions used in metal plasticity into the study of bulk solids. Since the strength of the material depends strongly on the hydrostatic stress, such an adaptation must include the first stress invariant into the yield function. Drucker and Prager [19] used this approach and showed the analogy between their yield function and the Mohr-Coulomb yield condition. However, their results did not truly represent the behavior of the material itself. Jenike and Shield [18] proposed a yield function based on the Mohr-Coulomb yield conditions. The strain-hardening behavior of the material is taken care of by varying the size of the yield envelop itself. The Mohr-Coulomb yield condition is written as

$$\left(\frac{\sigma_\theta - \sigma_r}{2}\right)^2 + \sigma_{r\theta}^2 = \left(\frac{\sigma_\theta + \sigma_r}{2}\right)^2 \sin^2\varphi \quad (4)$$

The condition of isotropy is used in the sense that the principal directions of stress and strain rates coincide. It should be mentioned that this condition is not universally accepted as has been discussed by Drescher [20] and Mandl and Fernandez Luque [21]. The isotropy condition is written as

$$\frac{\sigma_r - \sigma_\theta}{\sigma_{r\theta}} = \frac{\frac{\partial u}{\partial r} - \frac{1}{r}\frac{\partial v}{\partial \theta} - \frac{u}{r}}{\frac{1}{2}\left(\frac{\partial v}{\partial r} - \frac{v}{r} + \frac{1}{r}\frac{\partial u}{\partial \theta}\right)} \quad (5)$$

Analytical Solution

Using the stress expressions given by Sokolovskii [22], the stresses are written in terms of the mean stress σ and the stress angle ψ . Thus

$$\begin{aligned} \sigma_r &= \sigma(1 + \sin\varphi \cos 2\psi) \\ \sigma_\theta &= \sigma(1 - \sin\varphi \cos 2\psi) \\ \sigma_{r\theta} &= \sigma \sin\varphi \sin 2\psi. \end{aligned} \quad (6)$$

Since the flow is axisymmetric the stress in the α direction is a principal stress; for a converging flow field, it is equal to the major principal stress. Thus $\sigma_\alpha = \sigma(1 + \sin\varphi)$.

Using a perturbation technique based on the angular position θ , the dependent variables σ , ψ , u , v are written as

$$\begin{aligned} \sigma &= \sigma_0 + \sigma_2\left(\frac{\theta}{\theta_w}\right)^2 + O(\theta^4) \\ \psi &= \frac{\pi}{2} + \gamma_1\left(\frac{\theta}{\theta_w}\right) + \gamma_3\left(\frac{\theta}{\theta_w}\right)^3 + O(\theta^5) \\ u &= u_0 + u_2\left(\frac{\theta}{\theta_w}\right)^2 + O(\theta^4) \\ v &= v_1\left(\frac{\theta}{\theta_w}\right) + v_3\left(\frac{\theta}{\theta_w}\right)^3 + O(\theta^5) \end{aligned} \quad (7)$$

Note that when $\theta = 0$, $\psi = \pi/2$ which means that the stress field is in the passive state. The different powers of θ in the expansion are prescribed by the symmetry of the flow field.

Substituting these expansions into the equations of flow, the different expansion sequences are obtained.

The order θ^0 terms come from the continuity equation and the r direction equations of motion; they are

$$\left. \begin{aligned} \frac{du_0}{dr} + 2\frac{u_0}{r} + \frac{2v_1}{r\theta_w} &= 0 \\ \rho u_0 \frac{du_0}{dr} + (1 - \sin\varphi) \frac{d\sigma_0}{dr} - 4\left(1 + \frac{\gamma_1}{\theta_w}\right) \frac{\sin\varphi}{r} \sigma_0 + \rho g &= 0 \end{aligned} \right\} \quad (8)$$

The isotropy condition and the θ direction equation of motion give the order θ^1 terms

$$\left. \begin{aligned} 2\gamma_1 \left[\frac{du_0}{dr} - \frac{u_0}{r} - \frac{v_1}{r\theta_w} \right] &= \frac{2u_2}{r\theta_w} - \frac{v_1}{r} + \frac{dv_1}{dr} \\ \text{and} \\ \rho \left[\frac{v_1^2}{r\theta_w} + u_0 \left(\frac{v_1}{r} + \frac{dv_1}{dr} \right) \right] - \rho g \theta_w - 2 \\ \times \sin\varphi \gamma_1 \frac{d\sigma_0}{dr} - \frac{\sigma_0 \sin\varphi}{r} \left[\frac{2\gamma_1^2}{\theta_w} + 6\gamma_1 \right] \\ + \frac{2}{r\theta_w} [\sigma_2(1 + \sin\varphi) - 2\sigma_0 \sin\varphi \gamma_1^2] &= 0 \end{aligned} \right\} \quad (9)$$

The order θ^2 terms in the continuity equation and the r direction equation of motion give

$$\left. \begin{aligned} & \frac{du_2}{dr} + 2\frac{u_2}{r} + \frac{4v_3}{r\theta_w} - \frac{v_1\theta_w}{3r} = 0 \\ & \rho \left[u_2 \frac{du_0}{dr} + \frac{2u_2v_1}{r\theta_w} - \frac{v_1^2}{r} + u_0 \frac{du_2}{dr} \right] - \rho g \frac{\theta_w^2}{2} + 2\gamma_1^2 \sin \varphi \frac{d\sigma_0}{dr} \\ & + (1 - \sin \varphi) \frac{d\sigma_2}{dr} - \frac{3 \sin \varphi}{r\theta_w} \left[2\sigma_2\gamma_1 \right. \\ & \left. + \sigma_0 \left(2\gamma_3 - \frac{4}{3}\gamma_1^3 \right) \right] - \frac{\sigma_2 \sin \varphi}{r} \left(4 + \frac{2\gamma_1}{\theta_w} \right) \\ & \left. + \frac{\sigma_0 \sin \varphi}{r} \left(6\gamma_1^2 - \frac{2\gamma_1\theta_w}{3} - \frac{2\gamma_3}{\theta_w} + \frac{4\gamma_1^3}{3\theta_w} \right) = 0 \right\} \quad (10) \end{aligned}$$

These equations are solved subject to the following boundary conditions imposed by the geometry of the problem.

Along the hopper wall, $\theta = \theta_w$, the stresses have to satisfy the yield condition

$$\frac{\sigma_{r\theta}}{\sigma_\theta} = -\tan \delta \quad (11)$$

where δ is the wall friction angle.

Using (1), the value of ψ along the wall is then determined by the equation

$$\sin \varphi \sin 2\psi_w = -\tan \delta (1 - \sin \varphi \cos 2\psi_w) \quad (12)$$

The normal velocity along the wall should be equal to zero. Thus $v_1 + v_3 + \dots = 0$.

The discussion on the free surface condition will be delayed until later.

If only the terms of the expansion up to order θ^2 only are retained, the expansions of v and ψ will only have one term. Thus

$$v = v_1 = 0 \quad \text{and} \quad \psi = \psi_w = \frac{\pi}{2} + \gamma_1 \quad \text{on} \quad \theta = \theta_w.$$

The equations are solved by simple integration, giving

$$u_0 = U \left(\frac{r_1}{r} \right)^2$$

and

$$\frac{\sigma_0}{\rho g r_1} = \frac{1}{(\omega - 1)(1 - \sin \varphi)} \left(\frac{r}{r_1} \right) - \frac{2F}{(\omega + 4)(1 - \sin \varphi)} \left(\frac{r}{r_1} \right)^{-4} + A \left(\frac{r}{r_1} \right)^\omega \quad (13)$$

where U and A are the constants of integration, $F = U^2/gr_1$ is a modified Froude number and

$$\omega = \frac{4 \sin \varphi}{(1 - \sin \varphi)} \left(1 + \frac{\gamma_w}{\theta_w} \right)$$

Substituting these expressions for u_0 and σ_0 into equations (10) will give expressions for u_2 and σ_2 as follows:

$$\begin{aligned} u_2 &= -3\gamma_w\theta_w U \left(\frac{r_1}{r} \right)^2 \\ \frac{\sigma_2}{\rho g r_1} &= \left[\frac{\gamma_w(4\theta_w + 3\gamma_w) \sin \varphi}{(\omega - 1)(1 - \sin^2 \varphi)} + \frac{\theta_w^2}{2(1 + \sin \varphi)} \right] \left(\frac{r}{r_1} \right) \\ &+ \frac{2\gamma_w(\theta_w - 3\gamma_w)F \sin \varphi}{(\omega + 4)(1 - \sin^2 \varphi)} \left(\frac{r}{r_1} \right)^{-4} \\ &+ \frac{A\gamma_w(\omega\theta_w + 3\theta_w + 3\gamma_w) \sin \varphi}{1 + \sin \varphi} \left(\frac{r}{r_1} \right)^\omega. \end{aligned} \quad (14)$$

Boundary Condition on the Free Surface

The analysis in this section is based on the work of Brennen and Pearce [6]. Along the free surfaces, the mean stress is equal to zero. This will give the condition on the expansion terms σ_0 and σ_2 . If these free surfaces are taken to be the circumferential surfaces at the upper and lower radius, then

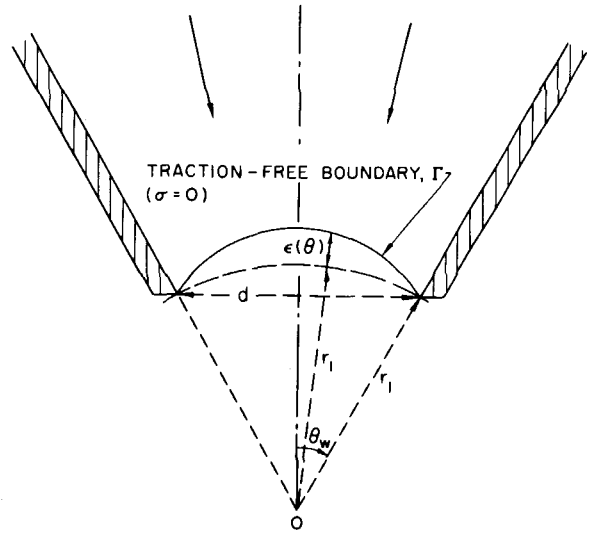


Fig. 2 Detail of the initially undetermined traction-free boundary, Γ , at discharge from the hopper

$$\sigma \Big|_{r_1} = \sigma_0 \Big|_{r_1} + \sigma_2 \Big|_{r_1} \left(\frac{\theta}{\theta_w} \right)^2 = 0$$

which gives

$$\sigma_0 \Big|_{r_1} = 0 \quad \text{and} \quad \sigma_2 \Big|_{r_1} = 0$$

However, the expressions of σ_0 and σ_2 have only two unknown constants (A and U) which are to be evaluated from the boundary conditions. Therefore, these four conditions on σ_0 and σ_2 along the free surfaces overspecify the problem. This implies that the free surfaces do not coincide with the circumferential surfaces and that their geometries will be determined by the condition of zero stress.

Following Brennen and Pearce [6], we let the free surface Γ and the circumferential lines be separated by a distance $\epsilon(\theta)$. The geometry is then as shown in Fig. 2. Assuming $\epsilon(\theta)$ to have a parabolic profile, we have

$$\epsilon(\theta) = \epsilon_1 \left[1 - \left(\frac{\theta}{\theta_w} \right)^2 \right]$$

The zero stress condition along Γ will be expanded in Taylor series from the stress along the circumferential line. Hence

$$\sigma \Big|_{\text{on } \Gamma} = \sigma \Big|_{r_1} + \epsilon_1 \left[1 - \left(\frac{\theta}{\theta_w} \right)^2 \right] \frac{d\sigma}{dr} \Big|_{r_1} = 0 \quad (15)$$

Substituting the expansion (7) for σ , we have

$$\begin{aligned} \sigma_0 \Big|_{r_1} + \epsilon_1 \frac{d\sigma_0}{dr} \Big|_{r_1} &= 0 \\ \sigma_2 \Big|_{r_1} + \epsilon_1 \frac{d\sigma_2}{dr} \Big|_{r_1} - \epsilon_1 \frac{d\sigma_0}{dr} \Big|_{r_1} &= 0 \end{aligned}$$

which are the terms of order θ^0 and θ^2 in (15). It can be seen then that ϵ_1 is of order θ_w^2 and to this order

$$\begin{aligned} (\sigma_0 + \sigma_2) \Big|_{r_1} &= 0 \\ \epsilon_1 &= \frac{\sigma_2 \Big|_{r_1}}{d\sigma_0/dr \Big|_{r_1}} \end{aligned}$$

This same condition can also be applied along the top surface. Evaluating the constants U and A in (13), we have

$$F = \frac{U^2}{gr_1} = \frac{\omega + 4}{2(\omega - 1)} \left[\frac{1 - \left(\frac{r_2}{r_1}\right)^{1-\omega}}{1 - \left(\frac{r_2}{r_1}\right)^{-4-\omega}} \right] \left[1 + \frac{\theta_w}{2(1 + \sin \varphi)} \right. \\ \left. \times (14\gamma_w \sin \varphi + 5\theta_w \sin \varphi - \theta_w) \right] \quad (16)$$

The exit velocity averaged over the exit area is given by

$$\bar{u} = \frac{\int_0^{\theta_w} u_{r=r_1} \sin \theta d\theta}{1 - \cos \theta_w}$$

or, in dimensionless form,

$$\frac{\bar{u}}{\sqrt{gD}} = \sqrt{\frac{F}{2 \sin \theta_w}} \left[1 - \frac{3\gamma_w \int_0^{\theta_w} \theta^2 \sin \theta d\theta}{(1 - \cos \theta_w)\theta_w} \right] \quad (17)$$

The nondimensional mean stress along the wall can be obtained from equations (13) and (14). Thus

$$\frac{\sigma}{\rho gr_1} = \left[\frac{(4\theta_w + 3\gamma_w)\gamma_w \sin \varphi + 1 + \sin \varphi}{(\omega - 1)(1 - \sin^2 \varphi)} + \frac{\theta_w^2}{2(1 + \sin \varphi)} \right] \left(\frac{r}{r_1} \right) \\ + F \left[\frac{2\gamma_w(\theta_w - 3\gamma_w) \sin \varphi - 2(1 + \sin \varphi)}{(\omega + 4)(1 - \sin^2 \varphi)} \right] \left(\frac{r}{r_1} \right)^{-4} \\ + A \left[1 + \frac{\gamma_w(\omega\theta_w + 3\theta_w + 3\gamma_w) \sin \varphi}{1 + \sin \varphi} \right] \left(\frac{r}{r_1} \right)^\omega \quad (18)$$

Some comments can be made about the solutions (17) and (18). First, the magnitude of the θ^2 terms are smaller than the θ^0 terms by factors of $\gamma_w\theta_w$, θ_w^2 or γ_w^2 . Thus the successive terms in the expansion decrease in magnitude and convergence of the regular expansion is expected. Second, the value of F (and therefore of \bar{u}) is independent of the ratio r_2/r_1 when the head of the material above the exit opening is sufficiently large. This is consistent with the well-known experimental observation of head independent flow.

Presentation of Results

In this section, the solution will be compared to some experimental data and to other analyses.

(a) **Comparison With Experimental Results.** Sand (686 μ m dia) and glass beads (610 μ m dia) were both used to obtain measurements of the mass flow rate in some conical hoppers. These granular materials are effectively cohesionless and have a size distribution which is fairly uniform. The measured internal friction angles were 31° for sand and 25° for the glass beads; their wall friction angle on an aluminum wall are 24.5° and 15°, respectively (see [6]). The bulk specific gravity of the flowing material (at critical void ratio) was 1.5 for both materials. The materials used in the present experiments have a fairly small grain size; the interstitial air may therefore have some effects on the flow rate. This effect was studied by Crewdson, Ormond, and Nedderman [25] who found that, for particles with diameters below 500 μ m, the interstitial air will affect the mass flow rate.

Two sets of hoppers of different sizes were used. The first set consisted of four small hoppers of exit diameter 2.03 cm with heights ranging from 6.35 cm to 12.7 cm and half-wall angles from 10° to 40°. The second set consisted of four larger hoppers with heights ranging from 17.78 cm to 33 cm and half-wall angles varying from 10° to 35°; observations were made with exit diameters of 2.03 cm and 3.3 cm. The flow rate at different exit diameters will be compared to assess any effect of the discrete nature of the materials. Furthermore, a vertical supply bin was provided on top of the small hoppers during the experiments. Any effect that such a vertical bin might have on the flow rate will be assessed by comparing the data of the two sets of hoppers.

The experimental procedure consisted of measuring the weight of

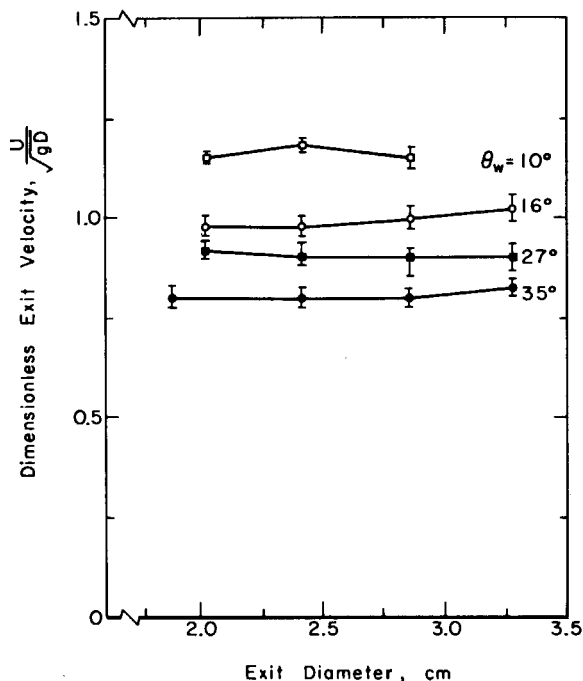


Fig. 3 Dimensionless exit velocity versus exit diameter for sand flowing in conical hoppers of various half-wall angles

material which flowed out of each hopper in a time interval of about 7 sec. Care was taken to ensure that there was sufficient material within the hopper so that the flow rate was constant with time. The resolution of the timing was ± 0.1 sec and that of the weighing about ± 0.1 gm. These resolutions will give an expected experimental error of about 15 percent. The measurements were fairly repeatable with the data points falling around 10 percent of the average value. Observations of the flow field for the sand and glass beads in a plane channel reveal very different behaviors according to the material used. Glass beads have a very uniform and radial flow field. Sands, on the other hand, flow in the hopper in a quite nonuniform way as previously observed by Lee, Cowin, and Templeton [26], Blair-Fish and Bransby [27] and Drescher, Cousens, and Bransby [28].

In Fig. 3 a plot of the dimensionless exit velocity versus the exit diameters for different hopper angles is presented. It can be seen that the results are fairly independent of the exit opening. This same behavior is also observed when an "empty annulus" is assumed to be present at the exit [29]. Using an effective diameter $\bar{D} = D - k$ where k can vary from 1 to 4 grain diameters, the dimensionless exit velocity is still independent of the effective diameter used in the experiments. This is an indication that the ratio D/d of the exit diameter to the particle size is sufficiently large in the present experiments for the "empty annulus" effect to be small.

The dimensionless exit velocities from both sets of hoppers are plotted versus the half-wall angle in Figs. 4 and 5 for sand and glass beads, respectively. Experimental data obtained by other authors are also presented. The data of Dening and Mehning [1] for potassium nitrate ($\varphi = 24^\circ$) compare well with the present experiments. However, their values for ammonium phosphate ($\varphi = 36^\circ$) are quite low; this may be due to substantial cohesive effects in this material. The data quoted by Williams [9] for sand ($\varphi = 34^\circ$, $\delta = 25^\circ$) and Nitram ($\varphi = 34^\circ$, $\delta = 19^\circ$) are also plotted on Fig. 4. These experiments were conducted in large size hoppers and the results correspond well with the present measurements for smaller hoppers. In these figures, the analytical results compared well with the experimental values up to a half-wall angle of about 30°.

The wall stress pattern is plotted in Fig. 6 and compared to the experimental results of Walker [16]. Agreement is reasonable even though the present values of stress are somewhat larger than the experimental values.

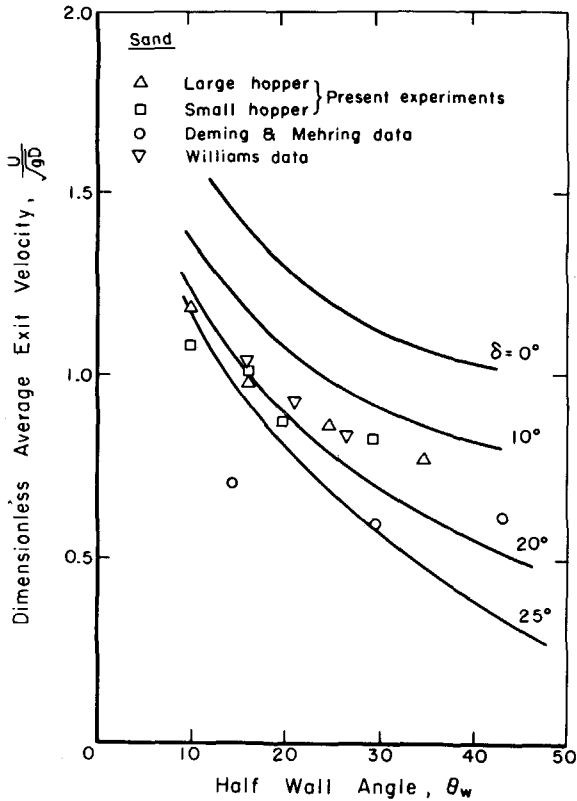


Fig. 4 The dimensionless average exit velocity for an internal friction angle of $\varphi = 35^\circ$ plotted against the hopper opening angle for various wall friction angles δ . Experimental data are for sand ($\varphi = 31^\circ$) with wall friction angle δ of 24.5°

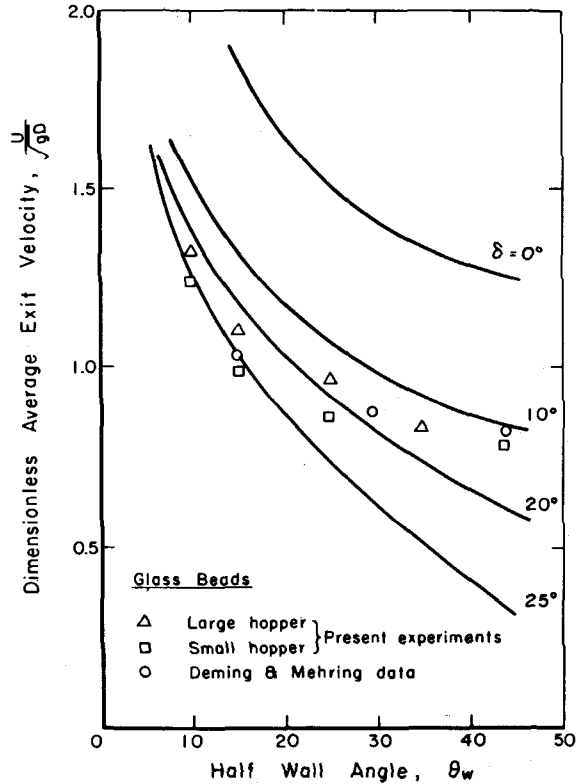


Fig. 5 Dimensionless average exit velocity for an internal friction angle of $\varphi = 25^\circ$ plotted against the hopper opening angle for various wall friction angles δ . Experimental data are for glass beads ($\varphi = 25^\circ$) with a wall friction angle φ of 15°

(b) Comparison With Other Analyses. In this section, the analytical expressions for the mass flow rate derived by Johanson, Brown, Williams, and Savage will be compared to the present solution.

Johanson [24] presented a semiempirical method for computing the flow rate of granular materials from hoppers. By considering a balance of forces acting on an arch across the hopper opening, he considered that the material would flow when the flow factor of the hopper was less than a critical value. The dimensionless exit velocity is obtained in the form

$$\frac{u}{\sqrt{gD}} = \frac{1}{\sqrt{4 \tan \theta_w}} \sqrt{1 - \frac{ff}{ffa}}$$

where

- ff = the hopper flow factor
- ffa = the critical value of the flow factor
- θ_w = the half-wall angle

This result is fairly general. It is dependent on both the hopper angle θ_w and the material property through the flow factor. However, the presence of the flow factor in the formula implies some degree of empiricism since this quantity must be determined independently. The upper limiting curve $u/\sqrt{gD} = (4 \tan \theta_w)^{-1/2}$ is presented in Fig. 7 since the flow factors for the hoppers used in the present experiments were not available.

Brown [4] used an energy principle to derive the mass flow rate of granular materials through an aperture. He suggested that the material would flow when the total potential and kinetic energies reached a minimum at a certain radius. Taking this radius to be that of the exit opening, he derived an upper limit of the dimensionless exit velocity as

$$\frac{u}{\sqrt{gD}} = \frac{2(1 - \cos^{3/2} \beta)}{3 \sin^{5/2} \beta}$$

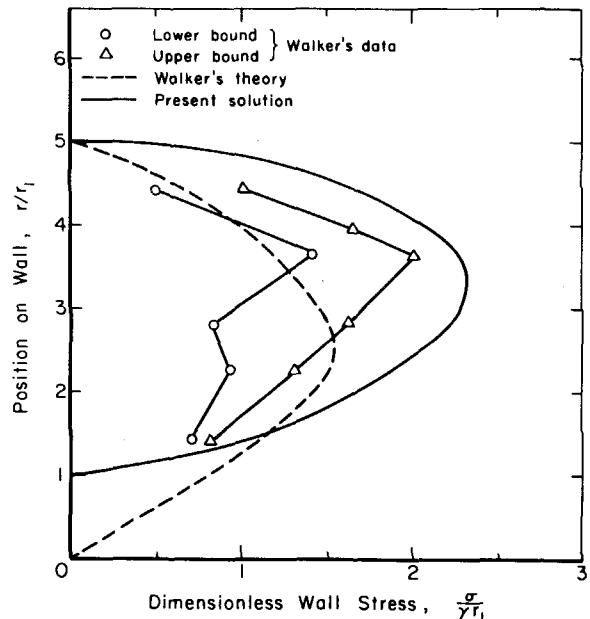


Fig. 6 Dimensionless wall stress plotted against the position along the wall for a material of internal friction angle $\varphi = 25^\circ$, a wall friction angle $\delta = 15^\circ$ and a hopper opening angle of $\theta_w = 30^\circ$. Also shown are the experimental measurements of Walker [7]

where β is the angle of the channel formed by the flowing material. For a mass flow hopper, β would be the hopper half-wall angle and is a simple geometric quantity. The results of this expression for the hopper used in the present experiments are included in Fig. 7.

Williams [9] derived the upper and lower limiting solutions by

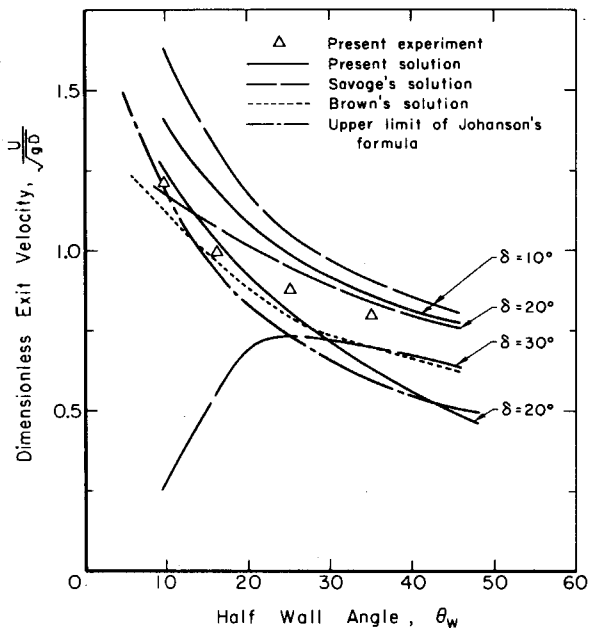


Fig. 7 Present solution is compared to other analytical results for an internal friction angle of 35° and various wall friction angles

solving the equations of the flow along the center line and the hopper wall, respectively.

Along the center line, he assumed that $\partial\psi/\partial\theta = 0$ which may not be justified. The expression of the center-line velocity is

$$v_0^2 = \frac{(k+1)}{(2k-3)} g \frac{r_1^5}{r^4}$$

Along the wall, the radial velocity is given by

$$v_w^2 = \frac{g}{2} \left(\cos \theta_w - \frac{\sin \varphi \sin 2\psi_w \sin \theta_w}{1 - \sin \varphi \cos 2\psi_w} \right) \left(\frac{B-4}{B+1} \right) \frac{r_0^5}{r^4}$$

where

$$k = \frac{1 + \sin \varphi}{1 - \sin \varphi}$$

and

$$B = \frac{k_2}{k_1}$$

where k_2 and k_1 are defined in his paper [9, page 250].

This solution is based on some assumptions which are important. For example, the values of $\partial\psi/\partial\theta$ on the center line and along the wall are approximations to the actual values. Also, the dependence of the radial velocity on the radial position θ taken to be $\cos^{-1/2} \theta$ is based on the observation of the frictionless wall solution and may not be representative of the actual velocity profile.

Savage [5] seems to have been the first author to systematically analyze the hopper flow problem by considering the complete equations of motion. His perturbation scheme is based on $\epsilon_1 = (\tan \delta)^{1/2}$ where δ is the wall friction angle and is based upon the limit process $(\tan \delta)/\theta_w \rightarrow 0$ as $\theta_w \rightarrow 0$. The results are given as

$$\frac{u}{\sqrt{gD}} = \left[\frac{k+1}{2(2k-3)\theta_w} \right]^{1/2} + \frac{\epsilon_1^2 k}{\theta_w} \left[\frac{1}{2} \{2(2k-3)(k+1)\theta_w\}^{-1/2} - \left[\frac{k+1}{2(2k-3)^3\theta_w} \right]^{1/2} \right]$$

where $k = (1 + \sin \varphi)/(1 - \sin \varphi)$.

Because of the aforementioned limit process it follows that this analysis and flow rate is invalid for wall angles, θ_w , less than about $\tan \delta$. This region of lack of validity is clearly demonstrated in Fig. 7. However provided $\tan \delta/\theta_w$ is small it would appear that Savage's

analysis yields results which are closer to the experimental data than the present analysis. In conclusion it would appear that the method presented in the present paper is appropriate for small hopper angles with discrepancies from the experiments occurring at larger θ_w ; on the other hand Savage's analysis may be more appropriate for small wall friction values and larger θ_w .

Conclusion

Treating the granular material as a perfectly plastic continuum, approximate solutions for the flow in a conical hopper were derived. It is seen that the continuum model describes the behavior of granular materials fairly well. It should be noted that the problem being studied is for a mass flow hopper only. Therefore, at large hopper angles, deviation between the theory and experiments is expected. Using the empirical criteria established by Jenike and Johanson [23] it is found that the upper limit of hopper angle for mass flow to exist is 20° for sand and about 25° for glass beads.

Acknowledgments

Support for this research was provided by the Union Carbide Corporation and by the National Science Foundation under Grant ENG. 76-15043.

References

- Deming, W. E., and Mehring, A. L., "The Gravitational Flow of Fertilizers and other Communitated Solids," *Industrial and Engineering Chemistry*, Vol. 21, 1929, p. 661.
- Rose, H. E., and Tanaka, T., "Rate of Discharge of Granular Materials From Bins and Hoppers," *Engineers*, London, Vol. 208, 1959, p. 465.
- Jenike, A. W., "Steady Gravity Flow of Frictional Cohesive Solids in Converging Channels," *ASME JOURNAL OF APPLIED MECHANICS*, Vol. 31, 1964, p. 5.
- Brown, R. L., "Minimum Energy Theorem for Flow of Dry Granular Through Apertures," *Nature*, London, Vol. 191, 1961, p. 458.
- Savage, S. B., "Gravity Flow of Cohesionless Bulk Solids in a Converging Conical Channel," *International Journal of Mechanical Science*, Vol. 9, 1963, p. 651.
- Brennen, C., and Pearce, J. C., "Granular Material Flow in Two-Dimensional Hoppers," *ASME JOURNAL OF APPLIED MECHANICS*, Vol. 45, 1978, p. 43.
- Davidson, J. F., and Nedderman, R. M., "The Hour-Glass Theory of Hopper Flow," *Transactions of the Institution of Chemical Engineers*, Vol. 51, 1973, pp. 29-35.
- Sullivan, W. N., "Heat Transfer to Flowing Granular Media," PhD Thesis, California Institute of Technology, Pasadena, Calif., 1972.
- Williams, J. C., "The Rate of Discharge of Coarse Granular Materials From Conical Mass Flow Hoppers," *Chemical Engineering Science*, Vol. 32, 1977, pp. 247-255.
- Walker, D. M., "An Approximate Theory for Pressure and Arching in Hoppers," *Chemical Engineering Science*, Vol. 21, 1966, p. 1975.
- Walters, J. K., "A Theoretical Analysis of Stresses in Axially Symmetric Hoppers and Bunkers," *Chemical Engineering Science*, Vol. 28, 1973, p. 779.
- Jenike, A. W., and Johanson, J. R., "Bin Loads," *Journal of The Structural Division, Proceedings of the ASCE*, Vol. 94, 1968, p. 1011.
- Jenike, A. W., Johanson, J. R., and Carson, J. W., "Bin Loads—Part 2: Concepts," *ASME Journal of Engineering for Industry*, Vol. 95, 1973, p. 1.
- Jenike, A. W., Johanson, J. R., and Carson, J. W., "Bin Loads—Part 3: Mass Flow Bins," *ASME Journal of Engineering for Industry*, Vol. 95, 1973, p. 6.
- Jenike, A. W., Johanson, J. R., and Carson, J. W., "Bin Loads—Part 4: Funnel Flow Bins," *ASME Journal of Engineering for Industry*, Vol. 95, 1973, p. 13.
- Walker, D. M., and Blanchard, M. H., "Pressures in Experimental Coal Hoppers," *Chemical Engineering Science*, Vol. 22, 1967, p. 1.1713.
- Cowin, S. C., "Theory of Static Loads in Bins," *ASME JOURNAL OF APPLIED MECHANICS*, Vol. 44, 1977, p. 409.
- Jenike, A. W., and Shield, R. T., "On the Plastic Flow of Coulomb Solids Beyond Original Failure," *ASME JOURNAL OF APPLIED MECHANICS*, Vol. 26, 1959, p. 599.
- Drucker, D. C., and Prager, W., "Soil Mechanics and Plastic Analysis of Limit Design," *Quarterly of Applied Mathematics*, Vol. 10, 1952-1953, p. 157.
- Drescher, A., "An Experimental Investigation of Flow Rules for Granular Materials Using Optically Sensitive Glass Particles," *Geotechnique*, Vol. 26.4, 1976, p. 591.
- Mandl, G., and Fernandez Luque, R., "Fully Developed Plastic Shear Flow of Granular Materials," *Geotechnique*, Vol. 20, 1970, p. 277.
- Sokolovskii, U. V., *Statics of Granular Media*, 1965, Pergamon Press.

23 Jenike, A. W., and Johanson, J. R., "Storage and Flow of Solids," Bulletin No. 123, 1964, Utah Engineering Experiment Station.

24 Johanson, J. R., "Method of Calculating the Rate of Discharge From Hoppers and Bins," *Transactions of the Society of Mining Engineers*, Vol. 232, 1965, p. 69.

25 Crewdson, B. J., Ormond, A. L., and Nedderman, R. M., "Air-Impeded Discharge of Fine Particles From a Hopper," *Powder Technology*, Vol. 16, 1977, pp. 197-207.

26 Lee, J., Cowin, S. C., and Templeton III, J. S., "An Experimental Study

of Flow Through Hoppers," *Transactions of the Society of Rheology*, Vol. 18, No. 2, 1974, pp. 247-269.

27 Blair-Fish, P. M., and Bransby, P. L., "Flow Patterns and Wall Stresses in a Mass-Flow Bunker," *ASME Journal of Engineering for Industry*, Vol. 95, 1973, pp. 17-26.

28 Drescher, A., Cousens, T. W., and Bransby, P. L., "Kinematics of the Mass Flow of Granular Materials Through a Plane Hopper," *Geotechnique*, Vol. 28, No. 1, 1978, pp. 27-42.

29 Brown, R. L., and Richards, J. C., *Principles of Powder Mechanics*, Pergamon Press, Oxford, 1970.

Readers Of The Journal Of Applied Mechanics Will Be Interested In: ASME's SI (Metric) Units Series

SI-1 ASME Orientation and Guide for Use of SI (Metric) Units — Eighth Edition

SI is the basic guide for all and should be used in conjunction with all other SI booklets which address themselves to specific fields.

1978 Bk. No. E00058 35 pp. \$2. Members \$1

SI-2 ASME Text Booklet: SI Units in Strength of Materials — Second Edition

The sections in this booklet cover: units and conversion factors; solved problems; and practice problems with answers. The tables cover: principal quantities encountered in strength of materials and their units; derived units; commonly used conversion factors; and average physical properties of common materials.

1976 Bk. No. E00082 14 pp. \$3. Members \$1.50

SI-3 ASME Text Booklet: SI Units in Dynamics

This text covers units and conversion factors, solved problems and practice problems with answers. The tables cover principal quantities encountered in dynamics and their units, derived units and commonly used conversion factors.

1976 Bk. No. E00083 20 pp. \$4. Members \$2.

SI-4 ASME Text Booklet: SI Units in Thermodynamics

Prepared by: James W. Murdock and Leo T. Smith

The sections in this booklet cover: units and conversion factors; conversion techniques; solved problems; and practice problems with answers. The tables cover: properties of selected gases at 101.3kPa and 20°C; principal quantities encountered in thermodynamics and their units; commonly used conversion factors; and SI unit prefixes.

1976 Bk. No. E00084 60 pp. \$6.50 Members \$3.25

SI-5 ASME Text Booklet: SI Units in Fluid Mechanics

Prepared by: James W. Murdock and Leo T. Smith

Covers units and conversion techniques, solved problems, and practice problems with answers. The tables cover fluid properties considered in the study of fluid mechanics, properties of selected liquids at 101.3kPa and 20°C, dimensionless numbers used in the study of fluid mechanics, principal quantities encountered in fluid mechanics and their units, derived units, commonly used conversion factors, and SI unit prefixes.

1976 Bk. No. E00085 36 pp. \$5. Members \$2.50

SI-6 ASME Text Booklet: SI Units in Kinematics

The sections in this booklet cover: units and conversion factors; solved problems; and practice problems with answers. The tables cover principal quantities encountered in kinematics and their units; derived units; units in use with the international system; and commonly used conversion factors.

1976 Bk. No. E00086 14 pp. \$3. Members \$1.50

SI-7 ASME Text Booklet: SI units in Heat Transfer

Prepared by: James W. Murdock

Covers units and conversion factors, conversion techniques, solved problems and practice problems with answers. The tables cover principal quantities encountered in heat transfer and their units, derived units, commonly used conversion factors. SI unit prefixes, dimensionless numbers used in the study of heat transfer, properties of air at one atmosphere, properties of saturated water and properties of 316 stainless steel.

1977 Bk. No. E00087 36 pp. \$5. Members \$2.50

SI-8 ASME Text Booklet: SI Units in Vibration

The sections cover: units and conversion factors; solved problems; and practice problems with answers. Tables cover: principal quantities encountered in vibration and their units; derived units; length; velocity; acceleration; mass; mass moment of inertia; force; and force per unit of deformation of spring constant.

1976 Bk. No. E00088 13 pp. \$3. Members \$1.50

SI-10 Steam Charts

Author: James H. Potter

Thermodynamic properties of Steam, h-v, in Graphical Form for the Superheated Vapor and Liquid Conditions in both SI (Metric) and U.S. Customary Units.

One prime application of the Steam Charts is to offer a compact, portable device for calling up appropriate values of steam properties without resorting to computers. The Steam Charts will be of real help in the hands of design engineers, manufacturers of steam-raising and steam-using equipment, and in engineering offices generally.

1976 Bk. No. E00090 128 pp. \$25. Members \$12.50

Descriptions of other ASME volumes of interest appear on pages 523, 528, 550, 572, 586, 591, 596, 636, and 643.

Address Orders To:

Order Department • The American Society Of Mechanical Engineers • 345 East 47th Street, New York, N.Y. 10017

AM-26E